AD-A089 302 ARIZONA UNIV TUCSON DEPT OF CHEMISTRY F/G 17/5
DETERMINATION OF THE ULTRAVIOLET AND VISIBLE SPECTRAL RESPONSE --ETC(U)
AUG 80 H A LEWIS, M B DENTON N00014-75-C-0513
UNCLASSIFIED TR-25 NL

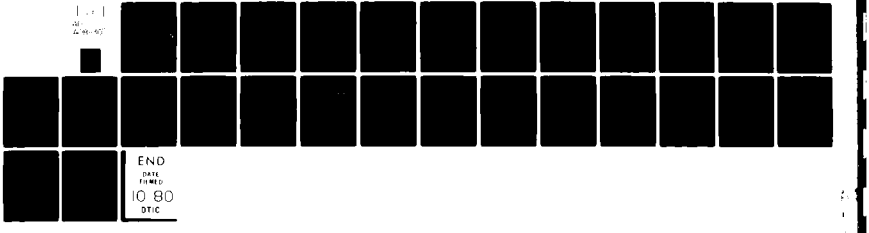

END
DATE FILMED
10 80
DTIC

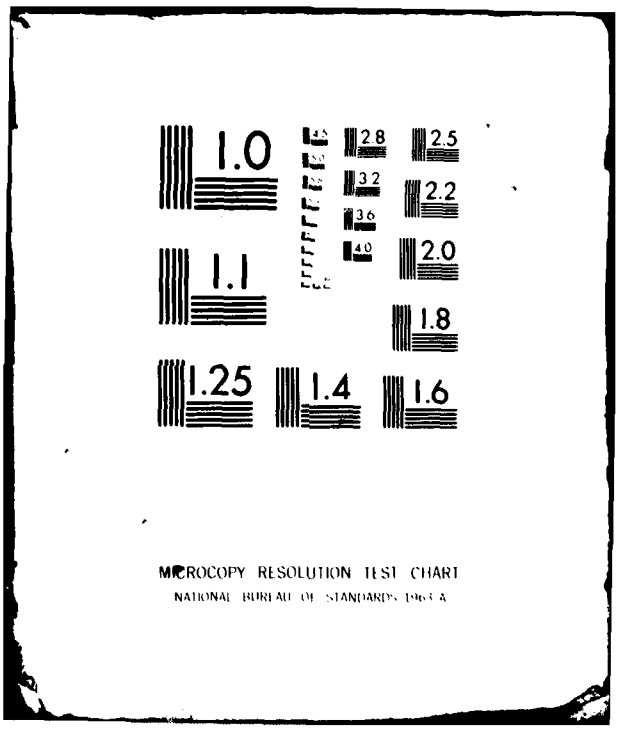
1.0
1.1
1.25
1.4
1.6
1.8
2.0
2.2
2.5
2.8
3.2
3.6
4.0
MICROCOPY RESOLUTION TEST CHART
NATIONAL BUREAU OF STANDARDS 1963-A

LEVEL II

12

OFFICE OF NAVAL RESEARCH
Contract N00014-75-C-0513
Task No. NR 051-549
Technical Report No. 25

DETERMINATION OF THE ULTRAVIOLET AND VISIBLE SPECTRAL RESPONSE OF A CHARGE - INJECTION DEVICE ARRAY DETECTOR

by

H. A. Lewis and M. B. Denton

Prepared for Publication

in

The Journal of Automatic Chemistry

Department of Chemistry
University of Arizona
Tucson, Arizona 85721

August, 1980

SECURITY CLASSIFICATION OF THIS PAGE (When Data Entered)

REPORT DOCUMENTATION PAGE

READ INSTRUCTIONS BEFORE COMPLETING FORM

1. REPORT NUMBER: 25
2. GOVT ACCESSION NO.: AD-A089302
3. RECIPIENT'S CATALOG NUMBER: 9

4. TITLE (and Subtitle): Determination of the Ultraviolet and Visible Spectral Response of a Charge-Injection Device Array Detector
5. TYPE OF REPORT & PERIOD COVERED: Interim rept.
6. PERFORMING ORG. REPORT NUMBER

7. AUTHOR(s): H. A. Lewis and M. B. Denton
8. CONTRACT OR GRANT NUMBER(s): N00014-75-C-0513

9. PERFORMING ORGANIZATION NAME AND ADDRESS
Department of Chemistry
University of Arizona
Tucson, Arizona 85721

10. PROGRAM ELEMENT, PROJECT, TASK AREA & WORK UNIT NUMBERS: NR 051-549

11. CONTROLLING OFFICE NAME AND ADDRESS
Office of Naval Research
Arlington, Virginia 22217

12. REPORT DATE: August 1980
13. NUMBER OF PAGES: 9

14. MONITORING AGENCY NAME & ADDRESS (if different from Controlling Office): TR-25

15. SECURITY CLASS. (of this report): Unclassified
15a. DECLASSIFICATION/DOWNGRADING SCHEDULE

16. DISTRIBUTION STATEMENT (of this Report)

Approved for Public Release: Distribution Unlimited

17. DISTRIBUTION STATEMENT (of the abstract entered in Block 20, if different from Report)

18. SUPPLEMENTARY NOTES

Prepared for Publication in The Journal of Automatic Chemistry

19. KEY WORDS (Continue on reverse side if necessary and identify by block number)

Charge-Injection Device, Solid State Imager, Array Detectors

20. ABSTRACT (Continue on reverse side if necessary and identify by block number)

The potential of charge-injection device (CID) electronic cameras as multichannel spectroscopic detectors is discussed. Data is presented giving the UV/visible spectral response of five CID sensors. This data shows that these sensors have the ultraviolet response necessary for their application as detectors in elemental analysis.

DD FORM 1 JAN 73 1473 EDITION OF 1 NOV 65 IS OBSOLETE
S/N 0102-LF-014-6601

033860

SECURITY CLASSIFICATION OF THIS PAGE (When Data Entered)

Determination of the Ultraviolet and Visible Spectral Response of a Charge - Injection Device Array Detector

H. A Lewis and M. B. Denton

Department of Chemistry
University of Arizona
Tucson, Arizona 85721

Abstract

The potential of charge-injection device (CID) electronic cameras as multichannel spectroscopic detectors is discussed. Data is presented giving the UV/visible spectral response of five CID sensors. This data shows that these sensors have the ultraviolet response necessary for their application as detectors in elemental analysis.

INTRODUCTION

One goal in atomic multielemental analysis is the ability to rapidly analyze a large number of elements over a wide concentration range. Thus an ideal spectrophotometer should detect many wavelengths simultaneously with wide spectral coverage, good sensitivity and a large linear dynamic range. Currently "direct readers" which employ individual slits and photomultiplier tube detectors (PMT) for each wavelength enjoy the greatest popularity. This is due to the numerous desirable characteristics of PMT's such as their high sensitivity and long, linear dynamic range. These instruments do suffer from several significant disadvantages such as a limited number of channels, difficulty in wavelength adjustment and high cost.

Recently work has been done in the adaptation of television type cameras as multichannel detectors in spectroscopic systems (1-3). These devices possess a large number of picture elements (pixels) to rapidly cover a wide wavelength range and yet are compact in size. Thus wavelength selection can be made electronically instead of through the manual adjustment of slit-photomultiplier tube assemblies. Some of the camera devices that have been applied are silicon vidicon tubes (4-8), silicon intensified target (SIT) tubes (9-12), image dissector (ID) tubes (8, 13-15), photodiode arrays (16-19), and charge-coupled device (CCD) arrays (20, 21).

The silicon vidicon, SIT, and ID all employ an electron beam to carry the video signal. Uncertainties in the control of this beam can hamper precise pixel selection in these devices. In addition the silicon

vidicon and the SIT suffer from cross-talk between pixels at high illumination levels (blooming) as well as incomplete removal of the charge signal on the target during readout (lag). In an effort to avoid these problems along with the mechanical limitations resulting from the delicate nature of vacuum tubes, solid-state cameras have been developed.

The photodiode array, CCD, and the charge-injection device (CID) (22-24) are solid state cameras that utilize sensors fabricated by employing integrated circuit fabrication technology. Photon generated charge is collected and stored in either reverse-biased photodiodes (the photodiode array) or in metal-oxide-semiconductor (MOS) capacitors (the CCD and the CID), resulting in virtually no lag, and digitally precise pixel addressing. The overall package is in general smaller, easier to cool and less expensive than the vacuum tube cameras. To date only the photodiode array and the CCD have been applied in spectroscopic systems.

In contrast to these approaches the charge-injection device has several unique features. The CID sensor consists of a discrete two-dimensional array of pixels, each of which is composed of a pair of silicon-type MOS capacitors. Figure 1 depicts a small portion of the row/column structure with field effect transistors (FETs), etc. Light striking the bulk silicon generates charge carriers which are stored underneath the capacitor with the greatest negative potential during the frame (integration) time (Figure 2A). This can best be understood by plotting potential well curves with stored charge underneath the capacitor plates (see Figure 2B). During the readout of each pixel, this charge is transferred from one of the capacitors to the other or to the substrate.

Several of the important readout concepts are diagrammed in Figures 3 and 4. Initially, each pixel site consisting of a row and column MOS capacitor can be thought of as having some initial bias potential V row (V_r) and V column (V_c) and an empty "well" (see Figure 3A). If both of these potentials are 15 volts negative and photons irradiate the surface, charge starts to collect in the well (see Figure 3B). If the row which crosses the particular pixel element about to be read out is clamped to zero volts, the quantities of charge stored under all the MOS capacitors within that row are transferred to each of the adjacent column electrodes (see Figure 3C). If a single column is now clamped to zero, the quantitites of charge stored under all of the capacitors in the column, exept for the pixel site which is in the process of being selected, merely move to their row capacitor (which are still negative).

However, for the one pixel site under selection, both the column and row capacitors are at zero potential, resulting in the stored charge being injected into the substrate (see Figure 3D). This current provides the video signal. Note that only the pixel at the intersection of the selected row and column has both capacitor plates at zero potential. All the other pixel sites have one or the other of the capacitors biased negative to store charge.

While this original mode of CID operation functions, it does not allow one of the most unique capabilities of the CID. To achieve nondestructible readout capability, a column potential is reduced (see Figure 4A) and charge accumulated under the row capacitor. For readout, the column containing the desired pixel is allowed to float and its potential is measured. Next, the row containing the pixel is clamped to zero volts and the charge in the selected pixel moves over to its column capacitor (see Figure 4B), changing

the "apparent" voltage on the entire column. This change in "apparent" column potential is dependent on the entire column capacitance and the charge accumulated in the selected pixel. If the row is returned to a more negative potential, the charge moves under it and the process can be repeated in a nondestructible readout mode, (i.e. V_c is allowed to float, measured, and the processes repeated, etc.). Destructive readout is accomplished by clamping the column to zero potential while the row is still zero (Figure 4D), causing the charge to be injected, as in Figure 3D.

With nondestructive readout capability blooming, which can still be a problem in the solid-state cameras, can be effectively eliminated by periodically scanning the array in a nondestructive readout mode to determine which pixels are near saturation. These pixels can be subsequently sampled in the destructive mode sufficiently often to prevent the leakage of charge into adjacent pixels. At the same time, pixels under low illumination can be allowed to integrate charge to maximize the signal-noise-ratio of weak lines. By averaging many repeated, nondestructive readouts of the signal stored in a pixel the readout noise, which is predominately due to white noise generated in the first stage of the preamplifier, can be reduced by the square root of the number of complete readouts (24).

CID devices can also be fabricated to provide random addressing of the array. With this capability only the desired pixels need be interrogated instead of sequentially scanning through the whole array as is required in most other solid-state devices. Thus, faster readout speeds are possible for rapid analysis.

On the basis of these characteristics, the CID shows definite potential as a multichannel detector for elemental analysis, provided it is able to detect light in the ultraviolet region where many elements have their strongest emission lines. The photodiode array meets this requirement but CCD's have been shown to be insensitive in this region (20) due to the absorption by the array electrodes that cover much of the sensors surface. The CID which has much smaller electrodes should have a sensitivity between that of the photodiode array and the CCD. Studies of the spectral response of CID's do not extend below 400 nm (23) or else indicate that the response quickly falls off in the UV (22). Unfortunately these detector arrays are normally manufactured with a glass window and the spectral response measurements were made using glass lenses (25). Thus since glass absorbs light below about 350 nm the UV response of the CID had not been conclusively evaluated. In the studies reported in this manuscript the spectral response for five CID sensors was measured from 190 to 800 nm using front surface mirrors and quartz optics to eliminate the absorption of glass. Five sensors were used to determine the extent of the variation in sensitivity from sensor to sensor.

EXPERIMENTAL

CID cameras are currently manufactured by General Electric (Syracuse, New York) and are commercially available in 128 x 128, 42 x 342 and 244 x 248 pixel arrays. Five CID 40B 128 x 128 sensors were obtained from General Electric with quartz faceplates instead of the standard optical glass. The faceplate covers and protects the pixel array which measures 5.85 x 5.85 mm. The sensors are mounted on 24 pin integrated circuit headers that plug into a socket on the front of a GE TN2200

camera electronics package. This electronic circuitry generates the necessary timing pulses to the chip as well as providing amplification of the video signal. It requires TTL clock and ± 15 volt power inputs that were supplied by a unit built in this laboratory. 40B CIDs have on-chip shift registers to provide sequential readout in a raster scan one-tenth that of the clock input. Additionally the standard TN2200 camera electronics package only provides for destructive readouts.

To determine their spectral response characteristics each sensor was evenly illuminated across the array with light from a Zeiss combination D_2/W lamp light source after passing through a monochrometer (see Figure 5). Two different monochrometers were used; a Jarell-Ash (Waltham, Mass.) model #82-410 1/4 meter with 4 mm slits and a GCA/McPherson (Acton, Mass.) model #EU-700 .35 meter with 2 mm slits. The Jarell-Ash was used in the 190-400 nm region because of its greater throughput so as to provide adequate light levels for the camera in the UV. With 4 mm slits the calculated bandwidth is 13 nm. As a result of the increased sensitivity of the CID's in the visible and a stray light problem observed with the Jarell-Ash above 500 nm the GCA/McPherson was used for the visible region measurements (400 to 800). With 2 mm slits the bandwidth of this monochrometer is 4 nm.

To calibrate the irradiance level of the light striking the sensors an EG & G (Salem, Mass.) model #550 radiometer with a silicon photodiode probe #550-2B was used. This probe was placed in the same position as the TN2200 camera and its output read in nanoamps. The current was then converted to $\mu W/cm^2$ by use of the calibration data supplied for the probe by the manufacturer. The output voltage signal from the camera for each sensor was measured vs. the wavelength setting

of the monochrometer with a Tektronix (Beaverton, Oregon) model #564 oscilloscope. The camera generates a timing pulse after each row of 128 pixels on the array has been read out. This pulse was used to trigger the scope so that the trace displayed each row output in rapid sequence. As there was a slight variation in illumination across the rows of the array the trace waveform was observed to oscillate vertically slightly as the different rows were read. The camera reading was taken from the central pixel of the row with the greatest output to insure that the same pixel was measured each time.

Also measured for each sensor was the potential output with the camera shielded from the light source (the dark potential). This potential is due to thermally generated charge in the sensor and was as much as one third of the saturation signal when low clock rates were used. For the UV measurements clock rates of 50 KHz, 100 KHz and 200 KHz were used depending upon the irradiance level falling on the camera. An Oriel (Stamford, Conn.) #772-3900 long-pass (>390 nm) filter was placed in front of the camera to determine the amount of visible wavelength stray light striking the camera. At all wavelengths except 190 nm only the dark potential was observed. The difference in signal was subtracted from measurements taken at 190 nm. Clock rates of 100 KHz, 200 KHz, 500 KHz, and 1 MHz were used for the visible region measurements because of the greater sensitivity and hence signal at these wavelengths. All measurements were corrected for differences in integration time.

Results and Discussion

The camera sensitivity vs. wavelength was calculated by dividing the net (light minus dark) camera signal by the net radiometer reading. As

the proportionality factor between the amount of charge stored in a pixel and the voltage output of the TN 2200's video amplifier is unknown it was impossible to determine absolute sensitivies. Thus only relative sensitivities are given here. The values obtained at the various clock rates were compensated for the difference in integration times by a simple multiplication factor. For example readings taken at 1 MHz were multiplied by ten to give an equivalent reading at 100 KHz. The data was then plotted as relative sensitivity vs. wavelength. It was noted that in the visible region measurements taken at different clock rates would sometimes give different response values at the same wavelength even after compensation for the difference in integration times. Figure 6 is an example of this phenomena. This effect was not observed in the UV data. It was thought that non-linearity in the transfer curve (a plot of camera output vs. input) of the CID's might be the cause. The transfer curves for the sensors were measured by using the GCA/McPherson monochrometer set to a constant (650 nm) wavelength and varying the light intensity striking the camera by adjusting the slit widths from 0 to 2 mm. Figure 7 shows a typical curve obtained. All of the curves showed a positive deviation from linearity at low signal levels and a slight negative deviation at high levels. The positive deviation has been observed in other CID devices (26) and can be eliminated through the use of a bias or "fat zero" charge (24). The deviation at high signal levels has also been seen before and is thought to be due to measuring the charge at the same time it is removed (i.e. destructive readout) (23). This should not be a problem when nondestructive readouts are used. When the non-linear regions of the transfer curve are ignored the observed variation in the sensitivity data disappear. This is illustrated in Figure 6 where a solid line connects the data that falls

in the linear region. Figure 8 is a plot of the final results of the combined UV/visible data for each of the five sensors. It shows that the maximum visible sensitivity is about seven times that of the UV region. Also, the variation in sensitivity from one sensor to the next is seen to be about ± 20% in the UV region. Assuming a typical CID sensitivity of .15 amps/Watt at 650 nm or a quantum efficiency of about 30% (23), the UV sensitivity would then be about .02 amps/Watt for a quantum efficiency in the range of 8 to 10%. Thus the CID possesses a satisfactory spectral response in order to function as a multichannel spectroscopic detector.

ACKNOWLEDGMENTS

This research was supported by a grant from the Office of Naval Research. We also wish to thank General Electric which loaned us several of their quartz faceplate CID sensors for this study.

References

1. Talmi, Y., Analytical Chemistry, 1975, 47, 658A.
2. Talmi, Y., Analytical Chemistry, 1975, 47, 699A.
3. Talmi, Y., Ed., "Multichannel Image Detectors," ACS Symposium Series Vol. 102, 1979, American Chemical Society, Washington, D.C.
4. Mitchell, D.G., Jackson, K.W., and Aldous, K.M., Analytical Chemistry, 1973, 45, 1215A.
5. Knapp, D.O., Omenetto, N., Hart, L.P., Plankey, F.W., and Winefordner, J.D., Analytical Chimica Acta, 1974, 69, 455.
6. Howell, N.G., and Morrison, G.H., Analytical Chemistry, 1977, 49, 106.
7. Felkel, Jr., H.L., and Pardue, H.L., Analytical Chemistry, 1977, 49, 1112.
8. Felkel, Jr., H.L., and Pardue, H.L., Analytical Chemistry, 1978, 50, 602.
9. Aldous, K.M., Mitchell, D.G., and Jackson, K.W., Analytical Chemistry, 1975, 47, 1034.
10. Chester, T.L., Haraguchi, H., Knapp, D.O., Messman, J.D., and Winefordner, J.D., Applied Spectroscopy, 1976, 30, 410.
11. Busch, K.W. and Malloy, B., Analytical Chemistry, 1979, 51, 670.
12. Furuta, N., McLeod, C.W., Haraguchi, H., and Fuwa, K., Applied Spectroscopy, 1980, 34, 211.
13. Golightly, D. W., Kniseley, R.N., and Fassel, V.A., Spectrochimica Acta B, 1970, 25, 451.
14. Danielsson, A. and Lindblom, P., Applied Spectroscopy, 1976, 30, 151.
15. Felkel, Jr., H.L. and Pardue, H.L. Clinical Chemistry, 1978, 24, 602.
16. Horlick, G. and Codding, E.G., Applied Spectroscopy, 1975, 29, 167.

17. Horlick, G., Applied Spectroscopy, 1976, 30, 113.

18. Yates, D.A. and Kuwana, T., Analytical Chemistry, 1976, 48, 510.

19. Chuang, F.S., Natusch, D.F.S., and O'Keefe, K.R., Analytical Chemistry, 1978, 50, 525.

20. Ratzlaff, K.L. and Paul, S.L., Applied Spectroscopy, 1979, 33, 240.

21. Ratzlaff, K.L., Analytical Chemistry, 1980, 52, 916.

22. Michon, G.J., Burke, H.K., and Brown, D.M., Proceedings of a Symposium on "Charge Coupled Device Technology for Scientific Imaging Applications", 1975, pp. 106-115.

23. Burke, H.K. and Michon, G.J., IEEE Transactions on Electron Devices, ED-23, 1976, 189.

24. Aikens, R.S., Lynds, C.R., and Nelson, R.E., Proceedings of the Society of Photo-Optical Instrumental Engineers, Vol. 78, "Low Light Level Devices", 1976, pp. 65-71.

25. Coates, P., General Electric Company, Syracuse, New York, personal communication, 1977.

26. Aikens, R.S., Photometric, Ltd., Tucson, Arizona, personal communication, 1980.

Figure Captions

Figure 1. Diagram of a small portion of a charge injection device array showing row and column FET selection and video preamplifier. Individual pixel (resolution) elements are comprised of a pair of metal oxide insulated capacitor plates. One on a row and one on a column. The pair of selection FETs on the columns allow separate control for voltage clamping and readout resulting in the capability to achieve the unique non-destructive mode.

Figure 2. A. Photons striking the bulk silicon generate positive charge carriers which are stored beneath the negatively biased capacitor plates.

B. The quantity of charge stored beneath the plates is often depicted in a "well" diagram. When the "well" is overfilled, charge spills out and is collected by surrounding pixel sights resulting in "blooming" and other undesired "crosstalk" effects.

Figure 3. The original injection mode readout for CIDs. Only the charge which is stored at the pixel site where both the column and row are clamped to zero is injected into the substrate.

Figure 4. The measuring sequence for combined non-destructive/destructive readout. In non-destructive mode the path B, C, float and measure is cycled through as many times as desired to improve signal to noise. (See description of operation in text.)

Figure 5. Schematic diagram of the experimental system used in determining the spectral response of the CID cameras.

Figure 6. Example of sensitivity data in the visible region obtained from one of the CID sensors using four different clock rates: 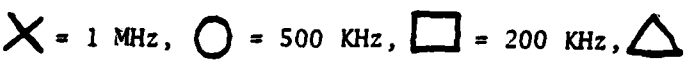 = 1 MHz, = 500 KHz, = 200 KHz, = 100 KHz

Figure 7. Plot of the transfer curve obtained from one of the CID sensors.

Figure 8. Plot of combined UV/visible sensitivity data obtained from the five CID cameras. The symbols  and denote the five different sensors.

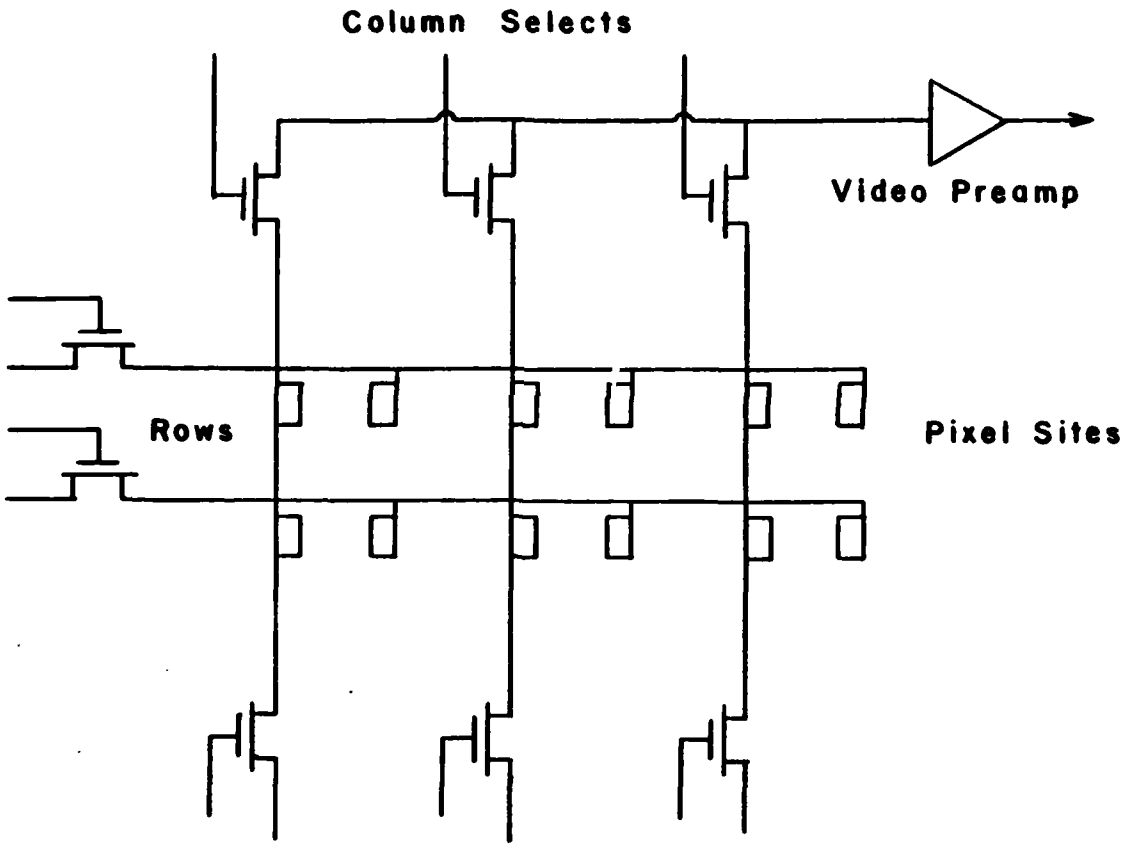
Column Selects
Video Preamp
Rows
Pixel Sites

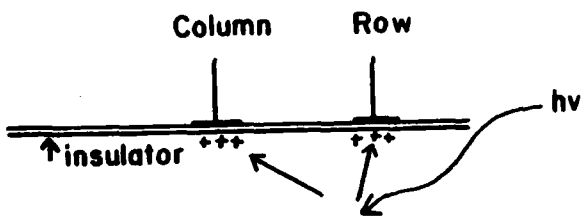

A

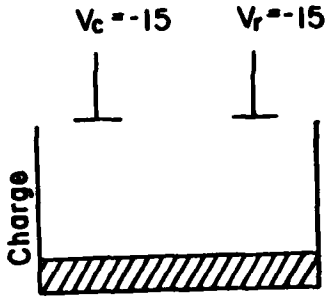

B

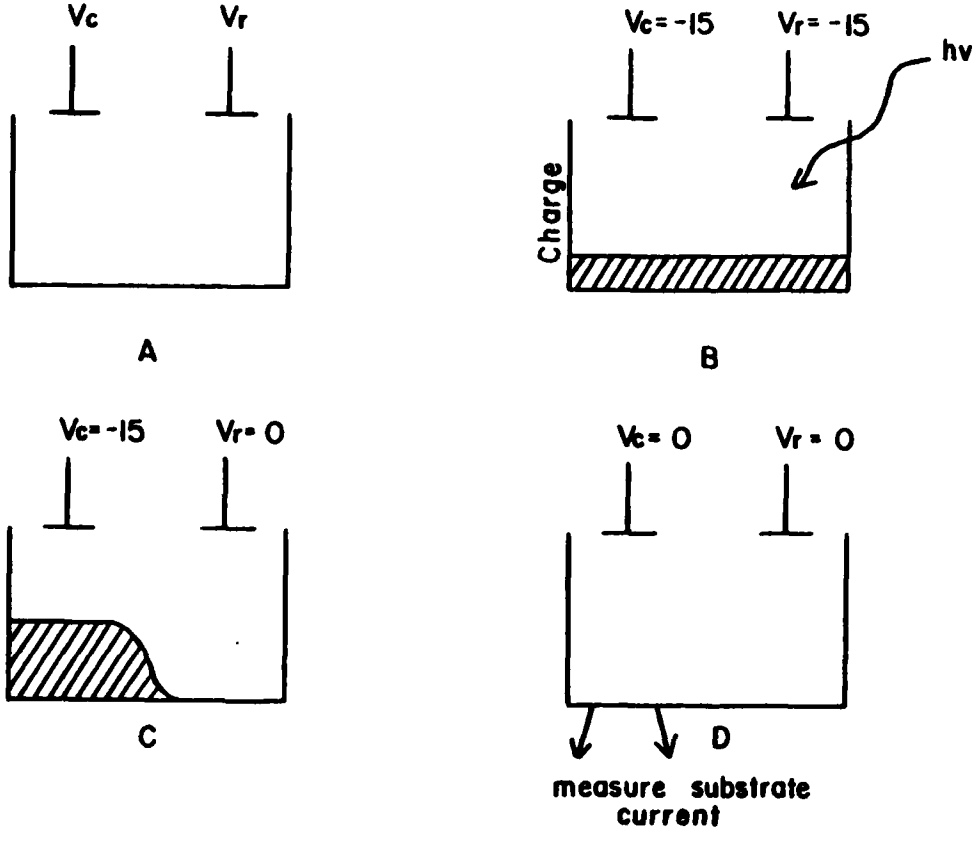
Vc
Vr
A
Vc= -15
Vr= -15
hv
Charge
B
Vc= -15
Vr= 0
C
Vc= 0
Vr = 0
D
measure substrate current

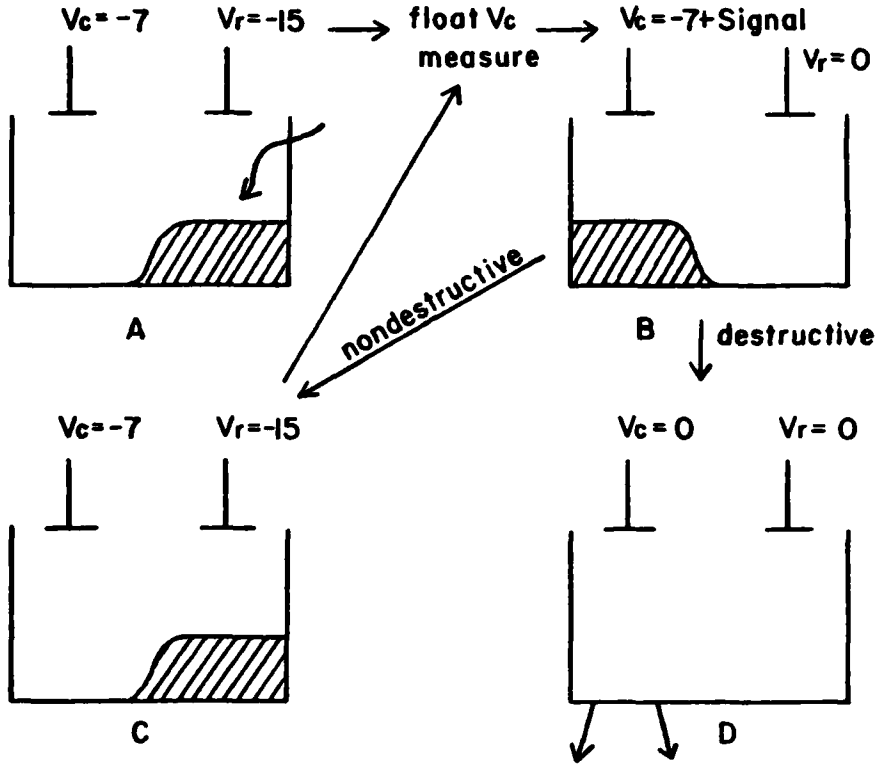
Vc = -7
Vr = -15
float Vc
measure
Vc = -7 + Signal
Vr = 0
A
B
nondestructive
destructive
Vc = -7
Vr = -15
Vc = 0
Vr = 0
C
D

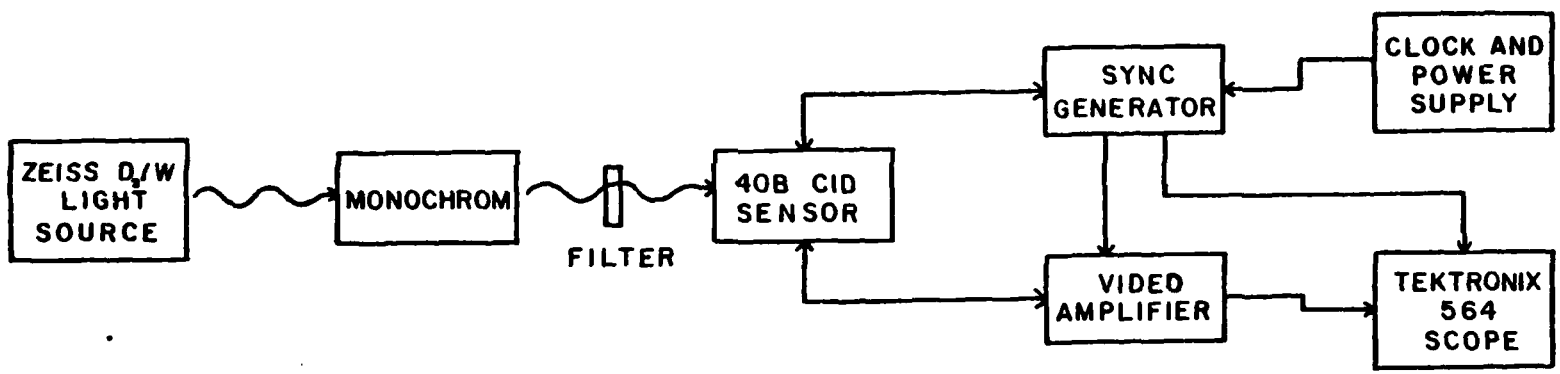
ZEISS D2/W LIGHT SOURCE
MONOCHROM
FILTER
40B CID SENSOR
SYNC GENERATOR
CLOCK AND POWER SUPPLY
VIDEO AMPLIFIER
TEKTRONIX 564 SCOPE

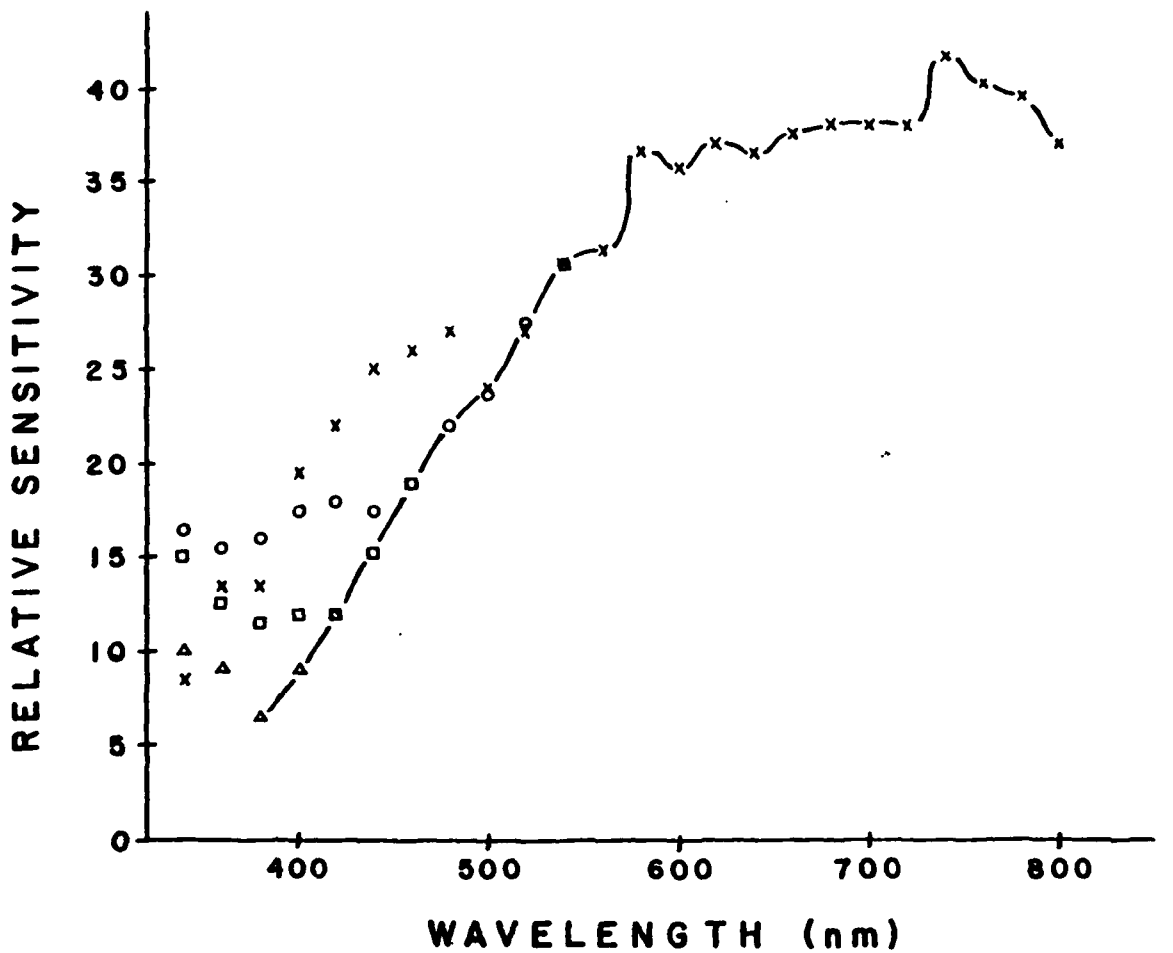
RELATIVE SENSITIVITY
0
5
10
15
20
25
30
35
40
400
500
600
700
800
WAVELENGTH (nm)

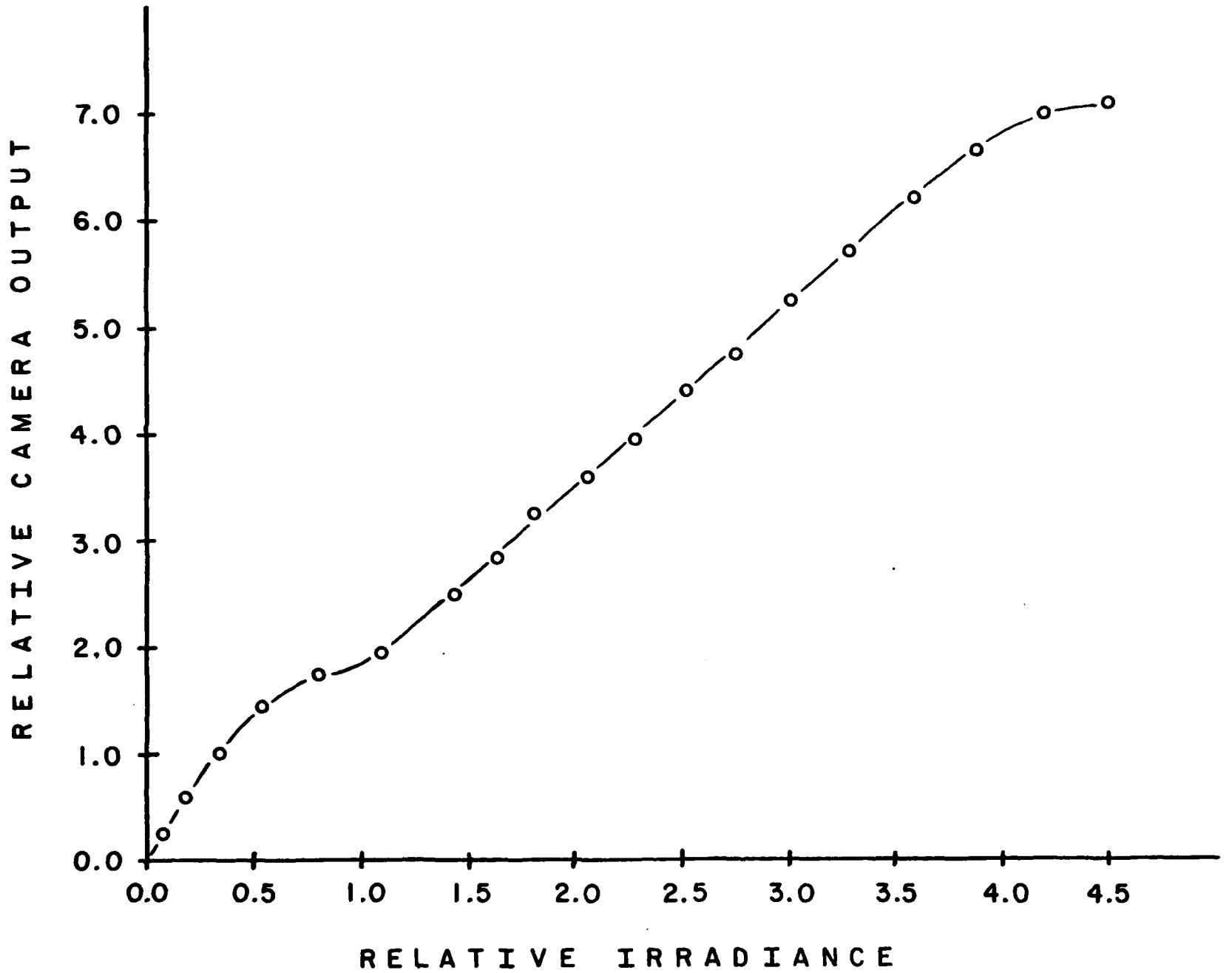
RELATIVE CAMERA OUTPUT
7.0
6.0
5.0
4.0
3.0
2.0
1.0
0.0
0.0
0.5
1.0
1.5
2.0
2.5
3.0
3.5
4.0
4.5
RELATIVE IRRADIANCE

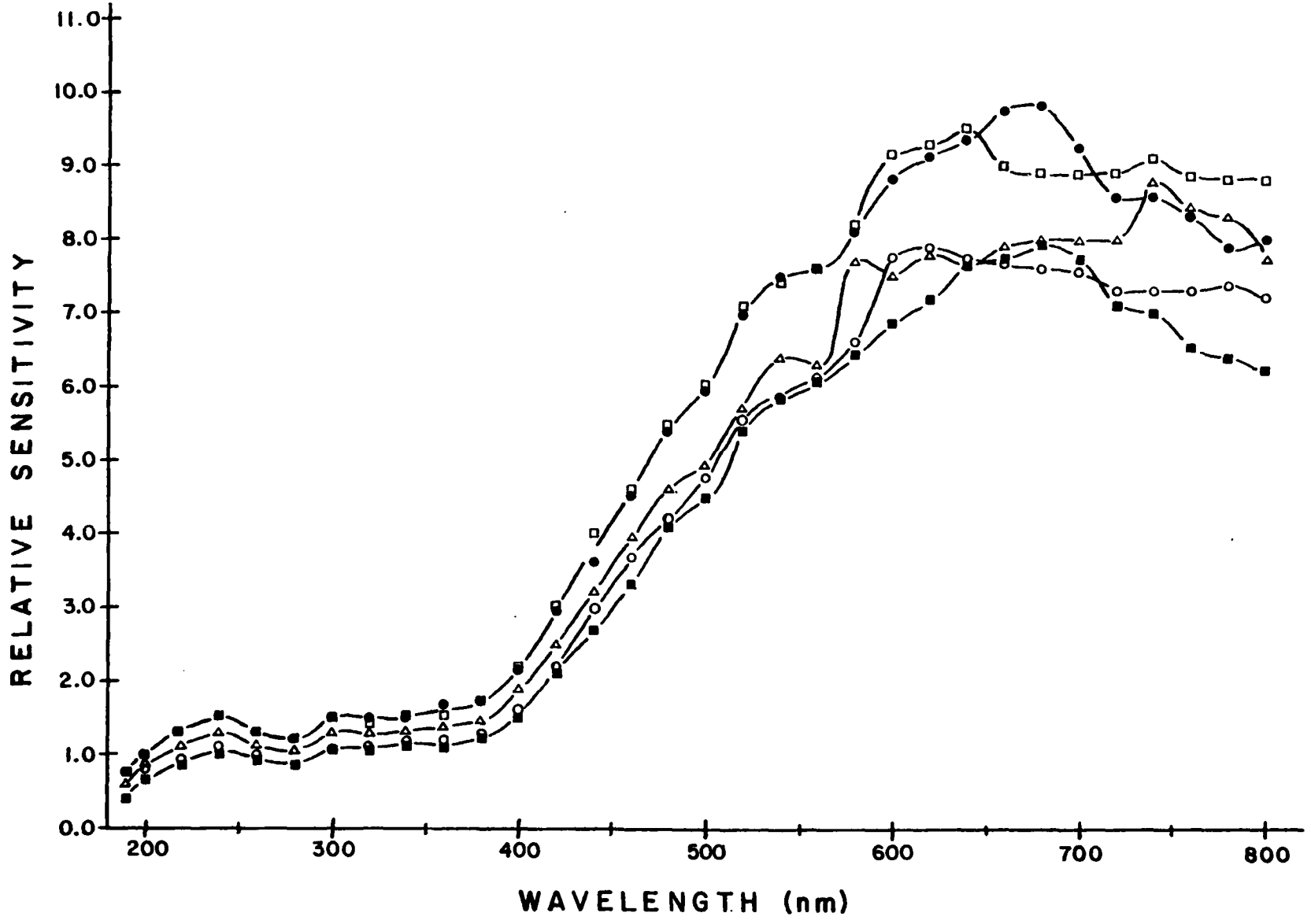
RELATIVE SENSITIVITY
11.0
10.0
9.0
8.0
7.0
6.0
5.0
4.0
3.0
2.0
1.0
0.0
200
300
400
500
600
700
800
WAVELENGTH (nm)

TECHNICAL REPORT DISTRIBUTION LIST, GEN

	No. Copies
Office of Naval Research Attn: Code 472 800 North Quincy Street Arlington, Virginia 22217	2
ONR Branch Office Attn: Dr. George Sandoz 536 S. Clark Street Chicago, Illinois 60605	1
ONR Area Office Attn: Scientific Dept. 715 Broadway New York, New York 10003	1
ONR Western Regional Office 1030 East Green Street Pasadena, California 91106	1
ONR Eastern/Central Regional Office Attn: Dr. L. H. Peebles Building 114, Section D 666 Summer Street Boston, Massachusetts 02210	1
Director, Naval Research Laboratory Attn: Code 6100 Washington, D.C. 20390	1
The Assistant Secretary of the Navy (RE&S) Department of the Navy Room 4E736, Pentagon Washington, D.C. 20350	1
Commander, Naval Air Systems Command Attn: Code 310C (H. Rosenwasser) Department of the Navy Washington, D.C. 20360	1
Defense Technical Information Center Building 5, Cameron Station Alexandria, Virginia 22314	12
Dr. Fred Saalfeld Chemistry Division, Code 6100 Naval Research Laboratory Washington, D.C. 20375	1
U.S. Army Research Office Attn: CRD-AA-IP P.O. Box 1211 Research Triangle Park, N.C. 27709	1
Naval Ocean Systems Center Attn: Mr. Joe McCartney San Diego, California 92152	1
Naval Weapons Center Attn: Dr. A. B. Amster, Chemistry Division China Lake, California 93555	1
Naval Civil Engineering Laboratory Attn: Dr. R. W. Drisko Port Hueneme, California 93401	1
Department of Physics & Chemistry Naval Postgraduate School Monterey, California 93940	1
Dr. A. L. Slafkosky Scientific Advisor Commandant of the Marine Corps (Code RD-1) Washington, D.C. 20380	1
Office of Naval Research Attn: Dr. Richard S. Miller 800 N. Quincy Street Arlington, Virginia 22217	1
Naval Ship Research and Development Center Attn: Dr. G. Bosmajian, Applied Chemistry Division Annapolis, Maryland 21401	1
Naval Ocean Systems Center Attn: Dr. S. Yamamoto, Marine Sciences Division San Diego, California 91232	1
Mr. John Boyle Materials Branch Naval Ship Engineering Center Philadelphia, Pennsylvania 19112	1

TECHNICAL REPORT DISTRIBUTION LIST, 051C

	No. Copies
~~Dr. M. B. Denton~~ ~~Department of Chemistry~~ ~~University of Arizona~~ ~~Tucson, Arizona 85721~~	1
Dr. R. A. Osteryoung Department of Chemistry State University of New York at Buffalo Buffalo, New York 14214	1
Dr. B. R. Kowalski Department of Chemistry University of Washington Seattle, Washington 98105	1
Dr. S. P. Perone Department of Chemistry Purdue University Lafayette, Indiana 47907	1
Dr. D. L. Venezky Naval Research Laboratory Code 6130 Washington, D.C. 20375	1
Dr. H. Freiser Department of Chemistry University of Arizona Tuscon, Arizona 85721	
Dr. Fred Saalfeld Naval Research Laboratory Code 6110 Washington, D.C. 20375	1
Dr. H. Chernoff Department of Mathematics Massachusetts Institute of Technology Cambridge, Massachusetts 02139	1
Dr. K. Wilson Department of Chemistry University of California, San Diego La Jolla, California	1
Dr. A. Zirino Naval Undersea Center San Diego, California 92132	1
Dr. John Duffin United States Naval Postgraduate School Monterey, California 93940	1
Dr. G. M. Hieftje Department of Chemistry Indiana University Bloomington, Indiana 47401	1
Dr. Victor L. Rehn Naval Weapons Center Code 3813 China Lake, California 93555	1
Dr. Christie G. Enke Michigan State University Department of Chemistry East Lansing, Michigan 48824	1
Dr. Kent Eisentraut, MBT Air Force Materials Laboratory Wright-Patterson AFB, Ohio 45433	1
Walter G. Cox, Code 3632 Naval Underwater Systems Center Building 148 Newport, Rhode Island 02840	1
Professor Isiah M. Warner Texas A&M University Department of Chemistry College Station, Texas 77840	1
Professor George H. Morrison Cornell University Department of Chemisty Ithaca, New York 14853	1
Dr. Rudolph J. Marcus Office of Naval Research Scientific Liaison Group American Embassy APO San Francisco 96503	1
Mr. James Kelley DTNSRDC Code 2803 Annapolis, Maryland 21402	1